Supporting Information for

RING-CONTRACTIVE AND -CLOSING SKELETAL REARRANGEMENT OF 1,1'-BINAPHTHALENE-2,2'-DIAMINES (BINAMS) INDUCED BY AN IODINE-CONTAINING OXIDANT: SYNTHESIS OF SPIRO[BENZO[*e*]INDOLE-1,1'-INDEN]-2-AMINES AND APPLICATION TO AN AIEE-ACTIVE BF_2 COMPLEX

Masato Okazaki, Kosuke Takahashi, Youhei Takeda,* and Satoshi Minakata*

Department of Applied Chemistry, Graduate School of Engineering,
Osaka University, Yamadaoka 2-1, Suita, Osaka 565-0871, Japan
E-mail: takeda@chem.eng.osaka-u.ac.jp; minakata@chem.eng.osaka-u.ac.jp

Table of Contents

Materials

6-Bromo-2-naphthol [CAS No. 15231-91-1] was prepared according to the procedures in literature.[SI] Commercial reagents were purchased from Sigma-Aldrich, TCI, and Wako Pure Chemical Industries, Ltd. and used as received. Solvents (fluorescence spectroscopic grade) were purchased from Nacalai Tesque Inc. and Kanto Chemical Co., Inc. for measurement of UV-vis and emission spectra.

Optimization Studies of Reaction Conditions

A Typical procedure for the optimization studies using 1a as a substrate

To a two-necked round-bottomed flask (50 mL) equipped with a three-way stopcock and a magnetic stir bar, was added 1,1'-binaphthalene-2,2'-diamine (**1a**) (56.8 mg, 0.2 mmol) under the air. The vessel was capped with a rubber septum, evacuated, and refilled with N_2 gas for three times, and an appropriate solvent (20 mL) was added through the septum. The resulting solution was cooled to –40 °C. To the solution, were added an additive (none, acid or base) and an appropriate oxidant under a stream of N_2 gas at –40 °C. The resulting solution was stirred for the indicated time before quenched with aqueous $Na_2S_2O_3$ solution (1.0 M, 20 mL), and the resulting mixture was extracted with CH_2Cl_2 (20 mL × 3). The combined organic extracts were dried over Na_2SO_4 and concentrated under vacuum to give the crude product. The yields of products were calculated by the integration of ^{1}H NMR signals of the crude product. Separation by flash column chromatography on NH silica gel gave product **2a**.

Note: t-BuOI was generated in situ from NaI and t-BuOCl as follows*: To a two-necked round-bottomed flask (50 mL) equipped with a magnetic stir bar, was added 1,1'-binaphthalene-2,2'-diamine (1a**) (56.8 mg, 0.2 mmol) and NaI (119.9 mg, 0.8 mmol) under the air. The flask was capped with a rubber septum, evacuated, and refilled with N_2 gas for three times, and then MeCN (20 mL) was added through the septum. The mixture was cooled to –40 °C. To the mixture, was added *t*-BuOCl (86.8 mg, 0.8 mmol) through the septum.

Table S1. The effect of solvents.

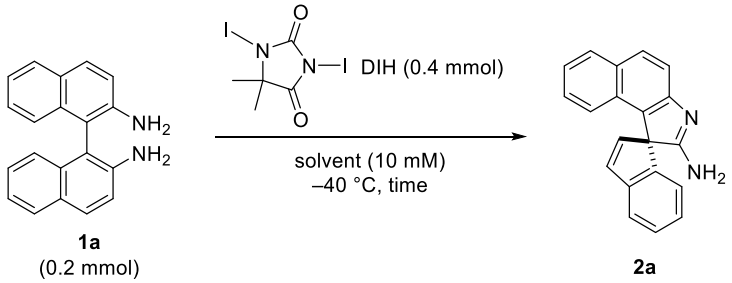

1a (0.2 mmol) **2a**

entry	solvent	time (h)	yield (%)[a]	recovery (%)[a]
1	MeOH	3	50[b]	19[b]
2	MeCN	3	47[b]	36[b]
3	MeCN	7	69[b]	17[b]
4	MeCN	12	43	7
5	THF	5	0	87
6	DMF	5	0	73
7	CH_2Cl_2	3	0	83
8	toluene	4	0	99
9	Et_2O	3	0	100
10	EtOH	5	38	49

[a] ^{1}H NMR yields. [b] isolated yield.

Table S2. The effect of halogen-containing oxidants.

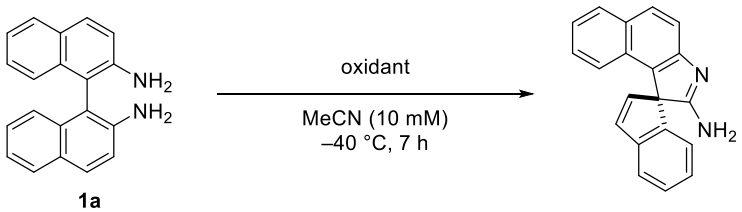

1a
(0.2 mmol)

2a

entry	oxidant (mmol)	yield (%)[a]	recovery (%)[a]
1	DIH (0.4)	69[b]	17[b]
2	DIH (0.2)	24	53
3	NIS (0.8)	45	49
4[c]	NIPy (0.8)	3	55
5	*t*-BuOI (0.8)	0	5
6	$PhI(OAc)_2$ (0.8)	0	47
7	$PhI(OTFA)_2$ (0.8)	0	31
8	DBH (0.4)	0	0
9	NBS (0.8)	0	0
10	DCH (0.4)	0	80
11	NCS (0.8)	0	62

[a] ^{1}H NMR yields. [b] isolated yield. [c] reaction time was 5 h.

structures of halogen-containing oxidants

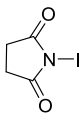

NIS
N-iodosuccinimide

NIPy
1-iodopyrrolidin-2-one

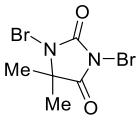

DBH
1,3-dibromo-5,5-dimethyl-hydantoin

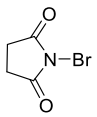

NBS
N-bromosuccinimide

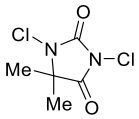

DCH
1,3-dichloro-5,5-dimethyl-hydantoin

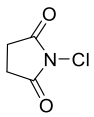

NCS
N-chlorosuccinimide

Table S3. The effect of other oxidants.

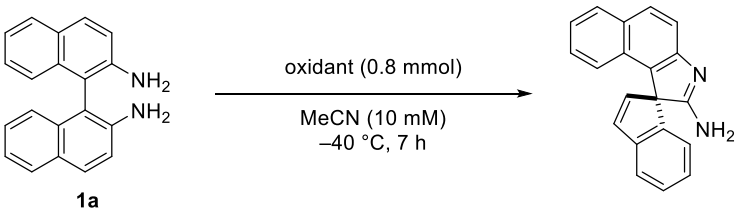

1a
(0.2 mmol)

2a

entry	oxidant	yield (%)[a]	recovery (%)[a]
1	$(NH_4)_2[Ce(NO_3)_6]$	0	0
2	$CuCl_2$ [b]	0	100
3	$CuSO_4•5H_2O$	0	100
4	DDQ	0	0
5	$Fe(NO)_3•9H_2O$	0	70
6	$FeCl_3•6H_2O$	0	100

[a] ^{1}H NMR yields. [b] *i*PrNH$_2$ (0.8 mmol) was added.

Table S4. The effect of bases.

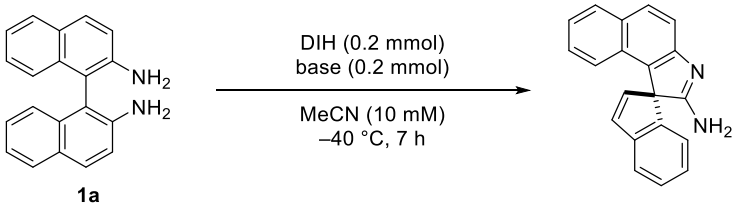

1a
(0.2 mmol)

2a

entry	base	yield (%)[a]	recovery (%)[a]
1	-	24	53
2	K_2CO_3	22	66
3	*t*-BuOK	0	100
4	HMDS	trace	100
5	DABCO	0	87
6	DBU	trace	88

[a] ^{1}H NMR yields.

structures of bases

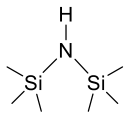

HMDS
1,1,1,3,3,3–hexamethyldisilazane

DABCO
1,4-diazabicyclo[2.2.2]octane

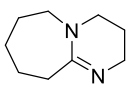

DBU
1,8–diazabicyclo[5.4.0]undec–7–ene

Table S5. The effect of acids.

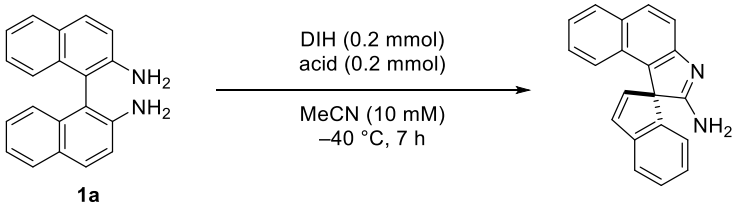

1a
(0.2 mmol)

2a

entry	base	yield (%) [a]	recovery (%)[a]
1	AcOH	0	35
2	CF_3COOH	0	43
3	$TsOH•H_2O$	0	58

[a] ^{1}H NMR yields.

Reaction of Spiro Product 2a with DIH (Equation S1)

To a two-necked round-bottomed flask (50 mL) equipped with a three-way stopcock and a magnetic stir bar, was added **2a** (56.4 mg, 0.2 mmol) under the air. The vessel was capped with a rubber septum, evacuated, and refilled with N_2 gas for three times, and acetonitrile (20 mL) was added through the septum. The resulting solution was cooled to –40 °C. To the solution, was added DIH (151.9 mg, 0.4 mmol) under a stream of N_2 gas at –40 °C. The resulting solution was stirred for 4 h before quenched with aqueous $Na_2S_2O_3$ solution (1.0 M, 20 mL), and the resulting mixture was extracted with CH_2Cl_2 (20 mL × 3). The combined organic extracts were dried over Na_2SO_4 and concentrated under vacuum to give the crude product. The yields of products were calculated by the integration of ^{1}H NMR signals of the crude product.

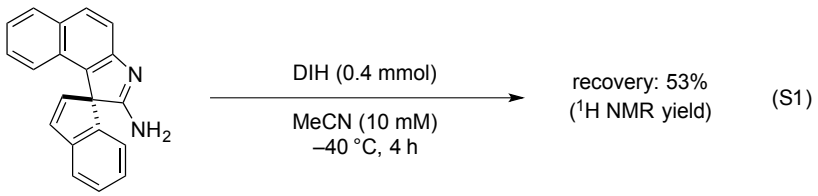

2a
(0.2 mmol)

(S1)

Reaction of 1a under the Conditions of Similar Type Rearrangements

The reaction was conducted according to the method for rearrangement of 1,1-binaphthalene-2,2'-diols (Equation S2).[S2]

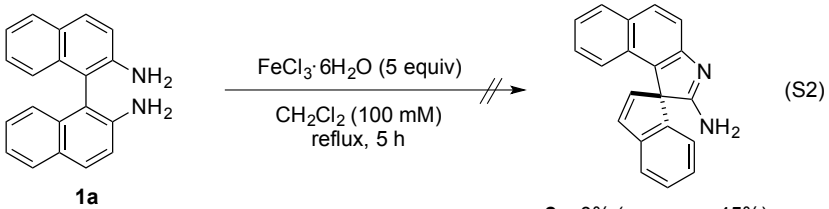

1a
(0.2 mmol)

2a, 0% (recovery: 45%)

(S2)

The reaction was conducted according to the method for rearrangement of 2'-amino-[1,1'-binaphthalen]-2-ol (Equation S3).[S3]

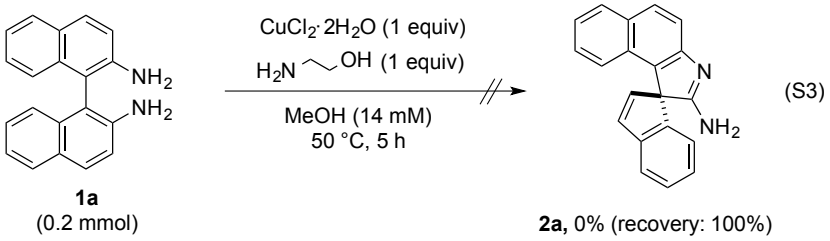

Investigation of the Substrate Scope of the Rearrangement

A typical procedure

To a two-necked round-bottomed flask (50 mL) equipped with a three-way stopcock and a magnetic stir bar, was added biaryldiamine **1** or **3** (0.1 mmol) under the air. The vessel was capped with a rubber septum, evacuated, and refilled with N_2 gas for three times, and an appropriate solvent (10 mL) was added through the septum. The resulting solution was cooled to the indicated temperature. To the solution, was added DIH (0.2 mmol) under a stream of N_2 gas at the indicated temperature. The resulting solution was stirred for the indicated time before quenched with aqueous $Na_2S_2O_3$ solution (1.0 M, 20 mL), and the resulting mixture was extracted with CH_2Cl_2 (20 mL × 3). The combined organic extracts were dried over Na_2SO_4 and concentrated under vacuum to give the crude product. The yields of products were calculated by the integration of ^{1}H NMR signals of the crude product. Separation by flash column chromatography on NH silica gel gave product **2**.

Table S6. Investigation of the rearrangement of biaryldiamine **1b**.

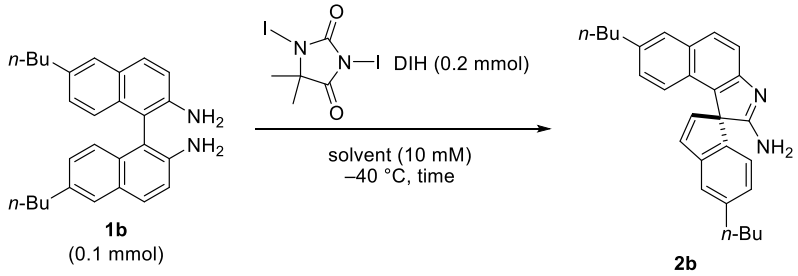

entry	solvent	time (h)	yield (%)[a]	recovery (%)[a]
1	MeCN	3	trace	31
2	MeOH	1	32	33
3	MeOH	3	40[b]	20[b]

[a] ^{1}H NMR yields. [b] isolated yield.

5',7-Di-*n*-butylspiro[benzo[*e*]indole-1,1'-inden]-2-amine (2b). Purified by NH silica gel column chromatography (eluent: hexane/EtOAc 5:5); brown solid; mp 65 °C (dec); R_f 0.15 (hexane/EtOAc

5:5 on an NH silica gel plate); ^{1}H NMR (400 MHz, $CDCl_3$) δ 0.89 (t, *J* = 7.2 Hz, 3H), 0.94 (t, *J* = 7.2 Hz, 3H), 1.28–1.43 (m, 4H), 1.54–1.67 (m, 4H), 2.60–2.68 (m, 4H), 6.35 (d, *J* = 5.2 Hz, 1H), 6.66 (d, *J* = 8.8 Hz, 1H), 6.81 (d, *J* = 7.6 Hz, 1H), 6.93–6.98 (m, 2H), 7.22 (d, *J* = 5.2 Hz, 1H), 7.36 (s, 1H), 7.53–7.55 (m, 2H), 7.74 (d, *J* = 8.8 Hz, 1H); *the peak assignable to N*H*$_2$ protons were difficult to detect due to the significantly broadened peak; ^{13}C NMR (100 MHz, $CDCl_3$) δ 13.9, 14.0, 22.3, 22.4, 33.5, 33.7, 35.6, 35.7, 70.2, 117.9, 121.1, 122.1, 122.7, 125.5, 127.1, 127.2, 127.5, 128.1, 129.0, 130.7, 134.9, 137.5, 138.1, 141.8, 143.2, 144.2, 154.9, 173.4; IR (ATR) *v* 3462, 2926, 2854, 1649, 1624, 1550, 1463, 1263, 821 cm^{-1}; MS (EI): *m/z* (relative intensity, %) 394 ($[M]^+$, 100), 351 ($[C_{25}H_{23}N_2]^+$, 60), 337 ($[C_{24}H_{21}N_2]^+$, 14), 308 ($[C_{22}H_{16}N_2]^+$, 10), 294 ($[C_{21}H_{14}N_2]^+$, 11); HRMS (EI): *m/z* calcd for $C_{28}H_{30}N_2$ (M) 394.2409, found 394.2409.

Table S7. Investigation of the rearrangement of biaryldiamine **1c**.

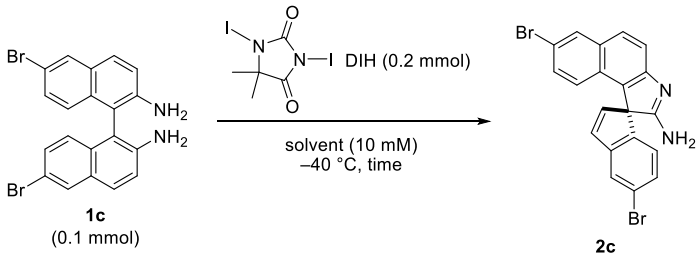

entry	solvent	time (h)	yield (%)[a]	recovery (%)[a]
1	MeCN	7	13[b]	71[b]
2	MeCN	12	5	31
3	MeOH	3	3	71
4	MeOH	7	5	37
5	MeOH	12	trace	15

[a] ^{1}H NMR yields. [b] isolated yield.

5',7-Dibromospiro[benzo[*e*]indole-1,1'-inden]-2-amine (2c). Purified by NH silica gel column chromatography (eluent: hexane/EtOAc 5:5 to 0:10); Pale yellow solid; mp 160 °C (dec.); R_f 0.24 (EtOAc on an NH silica gel plate); ^{1}H NMR (400 MHz, $CDCl_3$) δ 6.43 (d, *J* = 5.6 Hz, 1H), 6.55 (d, *J* = 8.8 Hz, 1H), 6.77 (d, *J* = 7.6 Hz, 1H), 7.19 (dd, *J* = 2.0, 9.2 Hz, 1H), 7.24 (d, *J* = 5.6 Hz, 1H), 7.26–7.28 (m, 1H), 7.59 (d, *J* = 8.0 Hz, 1H), 7.71 (d, *J* = 1.6 Hz, 1H), 7.74 (d, *J* = 8.8 Hz, 1H), 7.94 (d, *J* = 1.6 Hz, 1H); *the peak assignable to N*H*$_2$ protons were difficult to detect due to the significantly broadened peak; ^{13}C NMR (100 MHz, $CDCl_3$) δ 70.2, 116.9, 119.0, 122.6, 122.6, 124.3, 124.8, 125.5, 127.2, 129.1, 129.9, 130.0, 130.8, 131.6, 134.2, 139.4, 143.1, 145.8, 156.4, 172.8; IR (ATR) *v* 3441, 3078, 1651, 1629, 1548, 1504, 1450, 1271, 815, 761 cm^{-1}; MS (EI): *m/z* (relative intensity, %) 442 ($[M+4]^+$, 49), 440 ($[M+2]^+$, 100), 438 ($[M]^+$, 49), 359 ($[C_{20}H_{12}BrN_2]^+$, 58), 279 ($[C_{20}H_{11}N_2]^+$, 41), 237 ($[C_{19}H_9]^+$, 32), 140 ($[C_{10}H_6N]^+$, 32); HRMS (EI): *m/z* calcd for $C_{20}H_{12}Br_2N_2$ (M) 437.9367, found 437.9364.

Table S8. Investigation of the rearrangement of biaryldiamine **1d**.

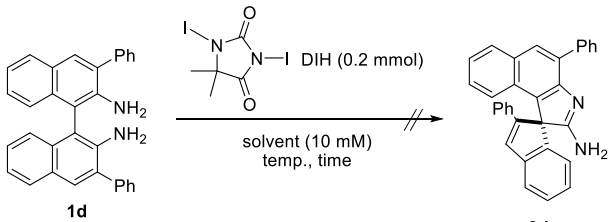

1d (0.1 mmol) **2d**

entry	solvent	temp. (°C)	time (h)	yield (%)[a]	recovery (%)[a]
1	MeCN	–40	48	0	87
2	MeOH	–40	3	0	100
3	MeCN	–30	3	0	76

[a] ^{1}H NMR yields.

Table S9. Investigation of the rearrangement of biaryldiamine **1e**.

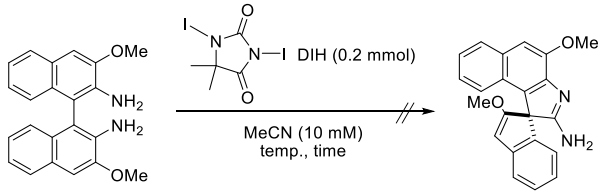

1e (0.1 mmol) **2e**

entry	temp. (°C)	time (h)	yield (%)[a]	recovery (%)[a]
1	–40	5	0	100
2	–30	3	0	86

[a] ^{1}H NMR yields.

Table S10. Investigation of the rearrangement of biaryldiamine **1f**.

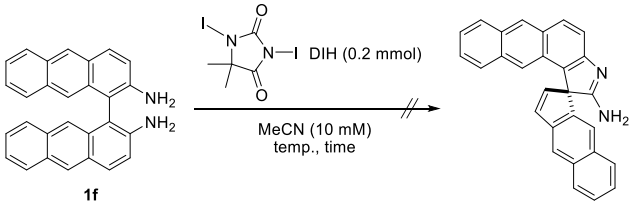

1f (0.1 mmol) **2f**

entry	temp. (°C)	time	yield (%)[a]	recovery (%)[a]
1	–40	7 h	0	0
2	–40	20 min	0	24
3	–78	30 min	0	71

[a] ^{1}H NMR yields.

Photo-induced Decomposition of Binaphthalene Azide 5

Acetonitrile was degassed through freeze-pump-thaw cycling for three times before use. To a quartz tube (150 mL) equipped with a three-way stopcock and a magnetic stir bar, was added **5** (62.0 mg, 0.2 mmol) under the air. The tube was capped with a rubber septum, evacuated, and refilled with N_2 gas for three times, and acetonitrile (20 mL) was added through the septum. The resulting solution was irradiated with UV light (Riko 400 W high pressure Hg lamp UVL-400HA) under N_2 atmosphere at –40 °C. After irradiation for 3 h, the solvent was concentrated under vacuum to give the crude product. Separation by flash column chromatography on NH silica gel gave the compound **2a**.

**Note: To maintain a constant reaction temperature, the apparatus was submerged in an acetonitrile/dry ice bath during the reaction.*

Derivatization of 2a to 6 and 7

The procedure for the synthesis of N-(spiro[benzo[e]indole-1,1'-inden]-2-yl)benzamide (6)

The *N*-acylation of **2a** was conducted according to a similar procedure described in the literature as follows:[S4] To a two-necked reaction tube (20 mL) equipped with a three-way stopcock and a magnetic stir bar, was added **2a** (56.4 mg, 0.2 mmol) under the air. The vessel was capped with a rubber septum, evacuated, and refilled with N_2 gas for three times, and Et_3N (22.2 mg, 0.22 mmol) and CH_2Cl_2 (2 mL) were added through the septum. The resulting solution was cooled to 0 °C. To the solution, was added benzoyl chloride (30.9 mg, 0.22 mmol) under a stream of N_2 gas, and the resulting solution was stirred for 30 min at 0 °C. The solution was warmed up to room temperature and stirred for 2 h. The solvent was concentrated under vacuum to give the crude product. Separation by flash column chromatography on silica gel (eluent: hexane/AcOEt 10:0–95:5) gave product the title compound **6** (39.4 mg, 51%). Pale yellow solid; mp 183 °C; R_f 0.33 (hexane/EtOAc 8:2); ^{1}H NMR (600 MHz, $CDCl_3$) δ 6.44 (d, J = 5.4 Hz, 1H), 6.90–6.92 (m, 2H), 7.09 (dd, J = 7.2, 7.2 Hz, 1H), 7.20 (dd, J = 7.2, 7.2 Hz, 1H), 7.29 (ddd, J = 0.6, 6.6, 7.8 Hz, 1H), 7.32–7.43 (m, 6H), 7.60 (d, J = 7.8 Hz, 1H), 7.82 (d, J = 8.4 Hz, 1H), 7.90 (d, J = 9.0 Hz, 1H), 8.08 (d, J = 7.2 Hz, 2H), 12.16 (br, 1H); ^{13}C NMR (150 MHz, $CDCl_3$) δ 68.6, 111.8, 121.2, 122.0, 122.1, 122.6, 124.5, 126.6, 127.5, 128.0, 128.2, 129.0, 129.3, 130.0, 130.4, 131.1, 132.1, 135.8, 136.8, 136.9, 140.8, 144.9, 145.9, 174.8, 180.0; IR (ATR) ν 3290, 3059, 1610, 1562, 1552, 1284, 1255, 1172, 997 cm^{-1}; MS (EI): *m/z* (relative intensity, %) 386 ([M]$^+$, 58), 309 ([$C_{21}H_{13}N_2O$]$^+$, 11), 281 ([$C_{20}H_{13}N_2$]$^+$, 17), 105 ([C_7H_5O]$^+$, 100), 77 ([C_6H_5]$^+$, 35); HRMS (EI): *m/z* calcd for $C_{27}H_{18}N_2O$ (M) 386.1419, found 386.1423.

The procedure for the synthesis of 8,8-difluoro-10-phenyl-8H-7λ^4,8λ^4-spiro[benzo[e][1,3,5,2]-oxadiazaborinino[3,4-a]indole-12,1'-indene] (7).

To a two-necked reaction tube (20 mL) equipped with a three-way stopcock and a magnetic stir bar, was added **6** (38.6 mg, 0.1 mmol) under the air. The vessel was capped with a rubber septum, evacuated, and refilled with N_2 gas for three times, and CH_2Cl_2 (3 mL), Et_3N (30.3 mg, 0.3 mmol) and $BF_3{\cdot}Et_2O$ (56.7 mg, 0.4 mmol) were added through the septum. The resulting solution was stirred for 24 h at room temperature. The solution was added CH_2Cl_2 (20 mL) and washed with water (20 mL × 3). The organic solvent was dried over $MgSO_4$ and concentrated under vacuum to give the crude product. Separation by flash column chromatography on silica gel (hexane/CH_2Cl_2 = 8:2–5:5) gave product **7** (18.6 mg, 43%). Further purification was carried out by recrystallization from *n*-hexane/$CHCl_3$. Yellow solid; mp 244 °C (dec.); R_f 0.25 (hexane/CH_2Cl_2 7:3); ^{1}H NMR (600 MHz, $CDCl_3$) δ 6.29 (d, *J* = 5.4 Hz, 1H), 6.83 (dd, *J* = 1.2, 7.2 Hz, 1H), 6.94 (dd, *J* = 1.2, 8.4 Hz, 1H), 7.12 (ddd, *J* = 1.2, 7.8, 8.4 Hz, 1H), 7.25–7.27 (m, 1H), 7.38–7.43 (m, 4H), 7.49 (dd, *J* = 0.6, 5.4 Hz, 1H), 7.57 (dd, *J* = 0.6, 8.4 Hz, 1H), 7.65 (d, *J* = 7.8 Hz, 1H), 7.89 (d, *J* = 8.4 Hz, 1H), 7.96 (d, *J* = 8.4 Hz, 1H), 8.02 (d, *J* = 9.0 Hz, 1H), 8.21 (dd, *J* = 1.2, 8.4 Hz, 2H); ^{13}C NMR (150 MHz, $CDCl_3$) δ 69.6, 115.3, 122.4, 122.5, 122.8, 125.7, 125.8, 127.1, 127.6, 128.5, 128.6, 129.0, 129.1, 130.9, 130.9, 131.1, 132.5, 133.4, 134.7, 138.1, 141.7, 141.8, 145.5, 173.1, 180.1; IR (ATR) *v* 3068, 2926, 1529, 1467, 1436, 1392, 1122, 1095, 1041, 987, 921, 806 cm^{-1}; ^{19}F NMR (564 MHz, $CDCl_3$) δ –136.6 (ddd, *J* = 16.9, 84.6, 107.1 Hz); ^{11}B NMR (192 MHz, $CDCl_3$) δ 0.66 (t, *J* = 13.4 Hz); MS (EI): *m/z* (relative intensity, %) 434 ([M]$^+$, 100), 265 ([$C_{20}H_{11}N$]$^+$, 39), 105 ([C_7H_5O]$^+$, 96), 77 ([C_6H_5]$^+$, 30); HRMS (EI): *m/z* calcd for $C_{27}H_{17}BF_2N_2O$ (M) 434.1402, found 434.1399.

Photophysical Properties

Solvents were purged with N_2 for 30 min before the measurements. UV-vis absorption and emission spectra were measured at room temperature using the solutions (1.0×10^{-5} M).

Table S11. Summary of photophysical properties of **2a**, **6**, and **7**.

	solvent	Absorption			Emission		
		λ_{abs} (nm)	ε ($M^{-1}cm^{-1}$)	λ_{edge} (nm)	λ_{ex} (nm)	λ_{em} (nm)	Φ_{FL}
2a	cyclohexane	254, 263, 272, 297, 308, 322, 344, 359	21846, 23192, 17601, 2691, 2899, 2691, 1967, 1656	379	260	391	0.02
2a	(solid)	-	-	-	300	-	<0.01
6	cyclohexane	255, 264, 282, 293, 340, 355	27987, 29695, 23594, 25221, 18712, 17248	408	300	-	<0.01
6	(solid)	-	-	-	300	470	0.05
7	cyclohexane	293, 305, 336, 350, 391	17078, 18537, 9440, 11499, 10384	470	300	527	0.06
7	toluene	295, 307, 352, 394	25102, 25506, 14932, 13398	480	300	547	0.03
7	THF	294, 305, 349, 390	23003, 25189, 15509, 13531	479	300	543	0.02
7	$CHCl_3$	295, 307, 351, 394	23914, 26191, 15563, 13665	485	300	544	0.03
7	CH_2Cl_2	295, 306, 350, 392	26813, 28224, 16430, 14213	481	300	553	0.02
7	acetone	348, 387	16624, 14236	484	350	552	0.01
7	DMF	295, 307, 350, 383	26788, 27446, 16448, 13723	491	300	571	0.01
7	(solid)	-	-	-	300	544	0.13

Lippert-Mataga plot[S5]

The Lippert-Mataga plot was constructed by using the relation

$$\Delta\nu = \nu_{abs} - \nu_{em} = -[2(\mu_e - \mu_g)^2/hca^3]\,\Delta f + \text{const.} \quad (4)$$

where $\Delta\nu$ is the Stokes shift, μ_g and μ_e are dipole moments in the ground state and excited state, respectively. a is Onsager cavity radius and Δf is the orientation polarizability of various solvents.

Table S12. Stokes shifts ($\Delta\nu$) of **7** and the orientation polarizability (Δf) of various solvents.

solvent	Δf	ν_{abs} (cm^{-1})	ν_{em} (cm^{-1})	$\Delta\nu$ (cm^{-1})
cyclohexane	–0.001	25575	18975	6600
toluene	0.0135	25380	18281	7099
THF	0.210	25641	18416	7225
$CHCl_3$	0.155	25380	18382	6998
CH_2Cl_2	0.218	25510	18083	7427
acetone	0.284	25839	18115	7724
DMF	0.276	26109	17513	8596

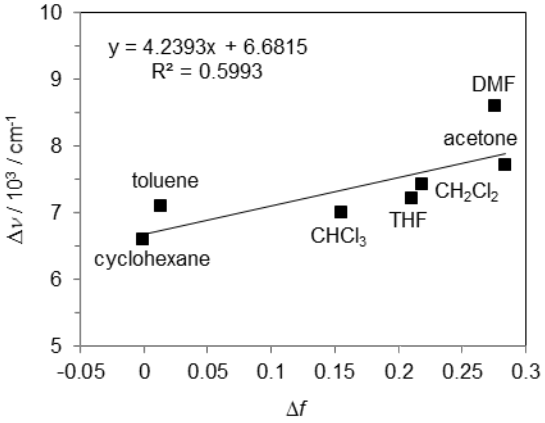

Figure S1. Lippert-Mataga plot of **7**.

X-ray Crystallographic data

The X-ray Diffraction data of the single crystal of **2a**, which was grown from an acetone solution, were collected on a Rigaku R-AXIS RAPID diffractometer with graphite monochromated CuKα radiation (λ = 1.54187 Å) to a $2\theta_{max}$ value of 136.4° at 123 K. The crystal structure was solved by direct methods (SIR92),[S6] expanded using Fourier techniques, and refined by full-matrix least-squares method on F^2 (SIR92)[S6]. The non-hydrogen atoms were refined anisotropically, and hydrogen atoms were refined using the riding model. The crystal data are summarized in Table S13. CCDC-1416916 contains the supplementary crystallographic data for **2a**, which are available free of charge from the Cambridge Crystallographic Data Center (CCDC) via www.ccdc.cam.ac.uk/data_request/cif.

Table S13. Summary of Crystallographic Data of **2a**.

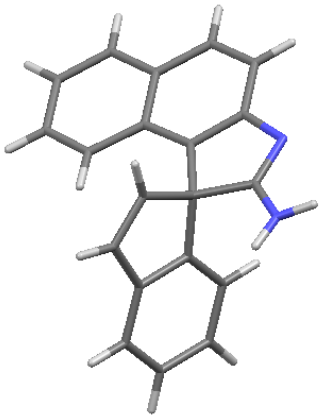

Empirical Formula	$C_{20}H_{14}N_2$	
Formula Weight	282.34	
Crystal System	monoclinic	
Space Group	$P2_1/c$ (#14)	
Unit cell dimensions	a = 12.8566(3) Å	α = 90 °
	b = 7.1822(2) Å	β = 101.868(2) °
	c = 16.5150(4) Å	γ = 90 °
V	1492.38(5) Å^3	
Z	4	
Density (calculated)	1.257 g/cm^3	
Absorption coefficient	5.774 cm^{-1}	
R_1 [I>2σ(I)]	0.0408	
wR_2 (all data)	0.1064	
Crystal size	0.600 × 0.350 × 0.150 mm	
Goodness-of-fit on F^2	1.069	
Reflections collected/unique	16175/2740 [R(int) = 0.0442]	

The X-ray Diffraction data of the single crystal of **7**, which was grown from a *n*-hexane/$CHCl_3$ mixed solution, were collected on a Rigaku R-AXIS RAPID diffractometer with graphite monochromated CuKα radiation (λ = 1.54187 Å) to a $2\theta_{max}$ value of 136.5° at 123 K. The crystal structure was solved by direct methods (SIR92),[S6] expanded using Fourier techniques, and refined by full-matrix least-squares method on F^2 (SIR92)[S6]. The non-hydrogen atoms were refined anisotropically, and hydrogen atoms were refined using the riding model. The crystal data are summarized in Table S14. CCDC-1416929 contains the supplementary crystallographic data for **7**, which are available free of charge from the Cambridge Crystallographic Data Center (CCDC) via www.ccdc.cam.ac.uk/data_request/cif.

Table S14. Summary of Crystallographic Data of **7**.

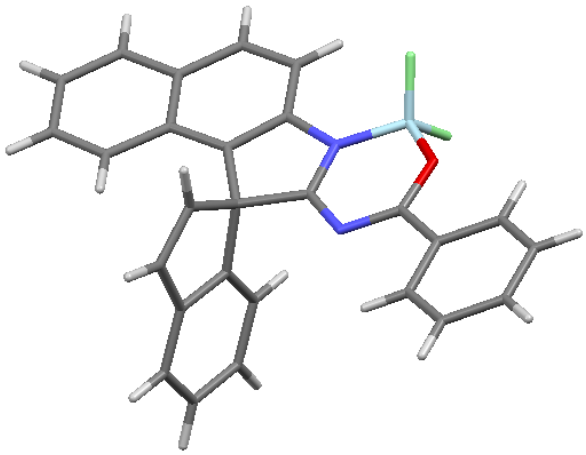

Empirical Formula	$C_{27}H_{17}BF_2N_2O$	
Formula Weight	434.25	
Crystal System	monoclinic	
Space Group	$P2_1/c$ (#14)	
Unit cell dimensions	a = 10.3671(4) Å	α = 90 °
	b = 10.9631(4) Å	β = 101.136(3) °
	c = 18.3325(5) Å	γ = 90 °
V	2044.4(2) Å^3	
Z	4	
Density (calculated)	1.411 g/cm^3	
Absorption coefficient	8.080 cm^{-1}	
R_1 [I>2σ(I)]	0.0627	
wR_2 (all data)	0.1838	
Crystal size	0.250 × 0.200 × 0.050 mm	
Goodness-of-fit on F^2	1.062	
Reflections collected/unique	21844/3708 [R(int) = 0.0692]	

Theoretical Studies

All the molecules were geometrically optimized by DFT method at the B3LYP/6-31G(d) level of theory using Gaussian 09 package.[S7] The excitation energies of the geometrically optimized molecules were calculated with the TD-DFT method at the same level of theory. Cartesian coordinates of the initial and optimized structures of **2a**, **6**, and **7** are listed below (Tables 15–20).

Table 15. Cartesian coordinates of the initial structure of **2a**.

Atom	*x*	*y*	*z*
N	9.742000	1.311000	7.754000
N	10.611000	-0.384000	6.414000
C	9.064000	1.101000	5.347000
C	9.847000	0.662000	6.596000
C	10.481000	-0.728000	5.046000
C	11.183000	-1.759000	4.395000
C	10.978000	-1.936000	3.051000
C	10.103000	-1.104000	2.308000
C	9.914000	-1.286000	0.914000
C	9.077000	-0.467000	0.209000
C	8.392000	0.585000	0.856000
C	8.545000	0.791000	2.199000
C	9.394000	-0.050000	2.969000
C	9.609000	0.092000	4.357000
C	7.558000	1.067000	5.559000
C	6.759000	0.035000	5.997000
C	5.389000	0.272000	6.132000
C	4.851000	1.510000	5.817000
C	5.658000	2.552000	5.374000
C	7.023000	2.327000	5.260000
C	8.135000	3.215000	4.896000
C	9.285000	2.552000	4.956000
H	9.213000	2.010000	7.821000
H	11.785000	-2.317000	4.874000
H	11.436000	-2.637000	2.604000
H	10.375000	-1.985000	0.465000
H	8.956000	-0.606000	-0.722000
H	7.821000	1.154000	0.354000
H	8.078000	1.503000	2.621000

H	7.130000	-0.815000	6.203000
H	4.820000	-0.422000	6.442000
H	3.915000	1.649000	5.907000
H	5.283000	3.397000	5.154000
H	8.045000	4.129000	4.653000
H	10.135000	2.935000	4.777000
H	10.265992	1.004107	8.548512

Table 16. Cartesian coordinates of the optimized structure of **2a**.

atom	*x*	*y*	*z*
N	9.710602	1.353135	7.741694
N	10.67058	–0.30327	6.386537
C	9.075996	1.133696	5.298265
C	9.856651	0.689149	6.562954
C	10.56729	–0.65164	5.022682
C	11.29044	–1.68573	4.39138
C	11.07844	–1.91153	3.048532
C	10.15529	–1.13524	2.293716
C	9.940322	–1.3743	0.910095
C	9.044017	–0.61998	0.187439
C	8.317121	0.416309	0.823657
C	8.496509	0.681052	2.162466
C	9.415924	–0.07959	2.938592
C	9.657711	0.128081	4.31508
C	7.566635	1.110857	5.521605
C	6.72637	0.046239	5.816558
C	5.360455	0.300996	5.999612
C	4.856072	1.60091	5.890916
C	5.701386	2.67481	5.593403
C	7.061842	2.424335	5.4072
C	8.180002	3.315682	5.075361
C	9.320013	2.604652	4.990354
H	8.862693	1.884201	7.883616
H	11.99461	–2.27909	4.966183
H	11.62425	–2.70212	2.538538
H	10.50183	–2.17189	0.428266
H	8.890863	–0.816201	–0.870269

H	7.610192	1.00727	0.246877
H	7.935173	1.477053	2.640989
H	7.11564	–0.96554	5.894105
H	4.686561	–0.52112	6.22432
H	3.79364	1.778204	6.03525
H	5.303633	3.682712	5.505424
H	8.084183	4.384809	4.915488
H	10.30928	2.982809	4.761165
H	10.09379	0.897371	8.559462

Table 17. Cartesian coordinates of the initial structure of **6**.

Atom	*x*	*y*	*z*
N	9.742000	1.311000	7.754000
N	10.611000	-0.384000	6.414000
C	9.064000	1.101000	5.347000
C	9.847000	0.662000	6.596000
C	10.481000	-0.728000	5.046000
C	11.183000	-1.759000	4.395000
C	10.978000	-1.936000	3.051000
C	10.103000	-1.104000	2.308000
C	9.914000	-1.286000	0.914000
C	9.077000	-0.467000	0.209000
C	8.392000	0.585000	0.856000
C	8.545000	0.791000	2.199000
C	9.394000	-0.050000	2.969000
C	9.609000	0.092000	4.357000
C	7.558000	1.067000	5.559000
C	6.759000	0.035000	5.997000
C	5.389000	0.272000	6.132000
C	4.851000	1.510000	5.817000
C	5.658000	2.552000	5.374000
C	7.023000	2.327000	5.260000
C	8.135000	3.215000	4.896000
C	9.285000	2.552000	4.956000
H	9.213000	2.010000	7.821000
H	11.785000	-2.317000	4.874000
H	11.436000	-2.637000	2.604000

H	10.375000	-1.985000	0.465000
H	8.956000	-0.606000	-0.722000
H	7.821000	1.154000	0.354000
H	8.078000	1.503000	2.621000
H	7.130000	-0.815000	6.203000
H	4.820000	-0.422000	6.442000
H	3.915000	1.649000	5.907000
H	5.283000	3.397000	5.154000
H	8.045000	4.129000	4.653000
H	10.135000	2.935000	4.777000
C	10.512268	0.859867	8.921933
O	11.296118	-0.174019	8.821737
C	10.399922	1.544680	10.139444
C	11.129954	1.118543	11.249368
C	9.558383	2.652344	10.241619
C	11.017895	1.799570	12.461337
H	11.792733	0.244782	11.168697
C	9.446929	3.334284	11.453619
H	8.983068	2.988449	9.366876
C	10.176393	2.908021	12.563448
H	11.592803	1.463364	13.336404
H	8.783648	4.207844	11.533773
H	10.088246	3.444862	13.519130

Table 18. Cartesian coordinates of the optimized structure of **6**.

atom	*x*	*y*	*z*
N	9.997882	1.021039	7.739176
N	10.80987	–0.64566	6.238431
C	9.300246	0.988395	5.321208
C	10.10906	0.399029	6.513877
C	10.5936	–0.90665	4.86531
C	11.18054	–1.96769	4.145211
C	10.87656	–2.096	2.807471
C	9.994902	–1.19327	2.148475
C	9.685665	–1.33201	0.768991
C	8.831212	–0.45552	0.139348
C	8.24266	0.60759	0.867433

C	8.516356	0.777441	2.205686
C	9.395943	–0.11027	2.886116
C	9.72845	–0.0054	4.255862
C	7.810317	1.090226	5.637418
C	6.890996	0.090811	5.924524
C	5.569854	0.459202	6.211043
C	5.187423	1.804754	6.213495
C	6.113219	2.813176	5.927042
C	7.429216	2.449456	5.636465
C	8.607733	3.253621	5.288665
C	9.666856	2.446667	5.082559
H	9.405487	1.840996	7.743347
H	11.85264	–2.65395	4.65016
H	11.3142	–2.90407	2.226045
H	10.14001	–2.15042	0.214901
H	8.605039	–0.57594	–0.91658
H	7.568124	1.29426	0.36259
H	8.061822	1.59422	2.757023
H	7.185487	–0.95517	5.920711
H	4.834612	–0.30973	6.4311
H	4.157622	2.069502	6.4377
H	5.810614	3.857289	5.926622
H	8.606431	4.335168	5.198155
H	10.67103	2.746114	4.805927
C	10.68278	0.729954	8.92528
O	11.56769	–0.10016	8.998802
C	10.2476	1.552889	10.10594
C	11.16368	1.685984	11.15897
C	8.983989	2.152298	10.2171
C	10.83443	2.428209	12.28974
H	12.12758	1.196195	11.06783
C	8.65271	2.88832	11.35505
H	8.234544	2.018178	9.441073
C	9.578847	3.033878	12.38905
H	11.55493	2.532991	13.09622
H	7.667749	3.339602	11.43648
H	9.320139	3.610047	13.27333

Table 19. Cartesian coordinates of the initial structure of **7.**

Atom	*x*	*y*	*z*
N	9.517044	1.043623	7.811647
C	9.155106	1.081854	5.257091
C	9.805379	0.614219	6.581392
C	10.715548	-0.643123	4.921066
C	11.527219	-1.549355	4.240856
C	11.221146	-1.831294	2.935914
C	10.100561	-1.220321	2.306207
C	9.761246	-1.547317	0.988768
C	8.689281	-0.956791	0.397335
C	7.911927	-0.014922	1.097212
C	8.223318	0.320833	2.375135
C	9.322829	-0.278211	2.995327
C	9.702610	0.030433	4.292656
C	7.627316	1.252601	5.325779
C	6.636428	0.275496	5.303112
C	5.300994	0.691218	5.491947
C	4.999082	2.064367	5.693293
C	6.025580	3.031486	5.653847
C	7.322280	2.585759	5.418175
C	8.602944	3.399662	5.186306
C	9.611875	2.523227	4.916198
H	12.358849	-2.016767	4.725596
H	11.826955	-2.520707	2.385838
H	10.345869	-2.261420	0.447268
H	8.434068	-1.210563	-0.610443
H	7.069809	0.439898	0.618512
H	7.631385	1.038925	2.903374
H	6.879204	-0.756284	5.155471
H	4.512065	-0.032160	5.487156
H	3.988110	2.367088	5.871058
H	5.813155	4.071111	5.791692
H	8.683976	4.466122	5.209307
H	10.570406	2.789620	4.522186
C	10.519841	0.824140	8.887542
O	11.561032	0.111556	8.690031

C	10.305922	1.479297	10.266284
C	11.239336	1.275297	11.292011
C	9.178795	2.280498	10.495361
C	11.047882	1.874634	12.544536
H	12.098653	0.661662	11.118942
C	8.988094	2.881460	11.747783
H	8.464272	2.433736	9.714059
C	9.923192	2.678904	12.771993
H	11.760669	1.717887	13.327180
H	8.128618	3.494878	11.921534
H	9.778477	3.138001	13.727574
N	10.716881	-0.268621	6.346836
B	11.623802	-0.846639	7.484881
F	12.994069	-1.001014	7.005716
F	11.107756	-2.147261	7.902541

Table 20. Cartesian coordinates of the optimized structure of **7**.

atom	*x*	*y*	*z*
N	9.664651	1.289048	7.791861
C	9.089491	1.098579	5.337049
C	9.812352	0.669044	6.619305
C	10.53498	–0.73748	5.025923
C	11.2613	–1.76945	4.401045
C	11.05351	–1.95911	3.053092
C	10.14843	–1.15019	2.308802
C	9.942283	–1.35898	0.919228
C	9.067731	–0.57178	0.20498
C	8.355645	0.466748	0.852767
C	8.527762	0.703039	2.19808
C	9.423931	–0.09201	2.963765
C	9.653098	0.086911	4.349127
C	7.57294	1.107397	5.538696
C	6.709555	0.060629	5.822649
C	5.34505	0.344359	5.972759
C	4.869611	1.652321	5.841577
C	5.742431	2.707168	5.554586
C	7.10058	2.42857	5.403666

C	8.24106	3.294957	5.089846
C	9.369983	2.567566	5.029375
H	11.96113	–2.37163	4.968629
H	11.59325	–2.74439	2.530059
H	10.49129	–2.15821	0.426876
H	8.920289	–0.74491	–0.8574
H	7.66602	1.081711	0.28082
H	7.978066	1.499212	2.688266
H	7.074902	–0.95809	5.921939
H	4.651019	–0.46232	6.191129
H	3.808157	1.851779	5.961307
H	5.367464	3.72223	5.452051
H	8.169387	4.364732	4.922436
H	10.37066	2.92599	4.819649
C	10.41243	0.845646	8.798856
O	11.23692	–0.1579	8.730186
C	10.33518	1.537477	10.09753
C	11.10925	1.092746	11.18205
C	9.484933	2.644819	10.2552
C	11.03252	1.749853	12.40673
H	11.76093	0.236216	11.05112
C	9.412206	3.295791	11.48289
H	8.893696	2.974414	9.408448
C	10.18513	2.850704	12.55932
H	11.63234	1.403607	13.24359
H	8.75327	4.151167	11.60262
H	10.12659	3.361206	13.51701
N	10.59836	–0.37527	6.392149
B	11.36863	–1.09511	7.55098
F	12.69313	–1.23597	7.222641
F	10.75732	-2.28613	7.855829

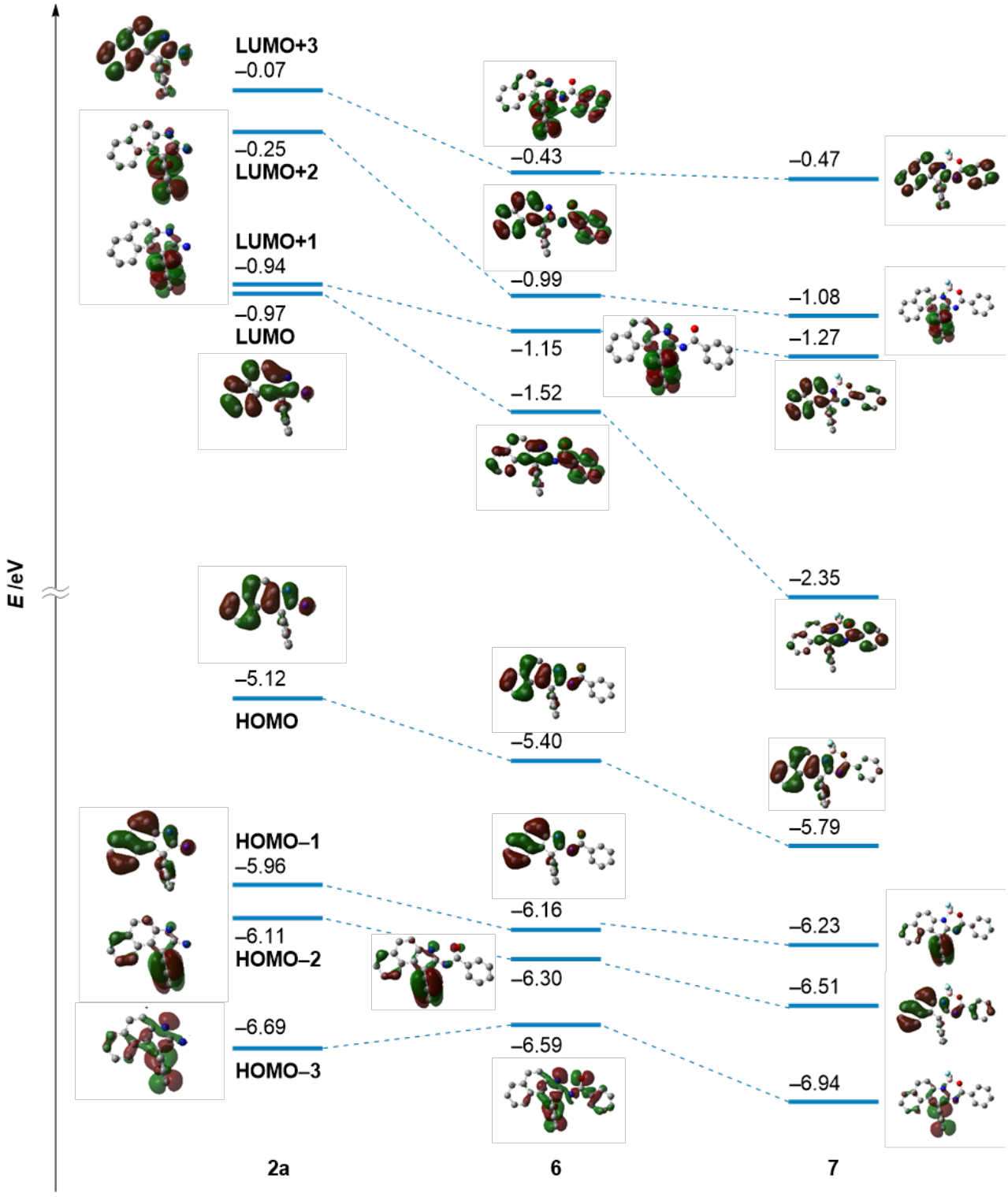

Figure 2. Energy diagram and molecular orbitals of **2a**, **6**, and **7**.

Table 21. Selected excitation energies and oscillator strength (*f*) of **2a**, **6**, and **7**.[a]

	2a	**6**	**7**
λ [nm] (*f*)	337.65 (0.0545)	361.61 (0.1860)	419.70 (0.1747)
transition mode	H→L (69%)	H→L (68%)	H→L (69%)
λ [nm] (*f*)	263.15 (0.1404)	300.84 (0.1725)	377.93 (0.1287)
transition mode	H–2→L+1 (53%)	H–1→L (50%)	H–1→L (68%)
λ [nm] (*f*)	256.35 (0.2794)	274.12 (0.1541)	342.22 (0.2420)
transition mode	H→L+3 (33%)	H–1→L+2 (41%)	H–2→L (67%)
λ [nm] (*f*)			302.63 (0.1733)
transition mode			H→L+1 (62%)

[a] The coefficient percentages of orbitals involved in the transitions are shown in parentheses.

NMR Charts

^{1}H NMR: (400 MHz, $CDCl_3$)

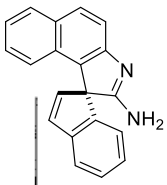

2a

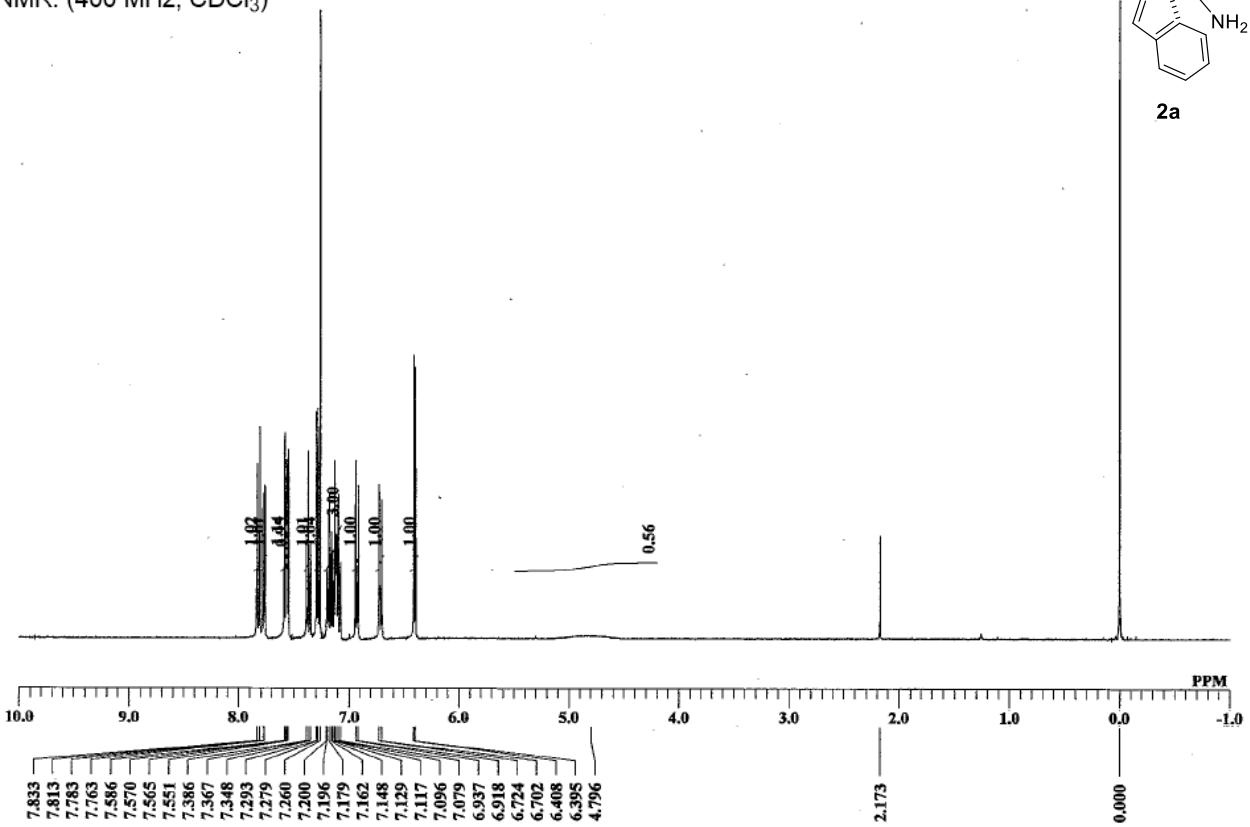

^{13}C NMR: (100 MHz, $CDCl_3$)

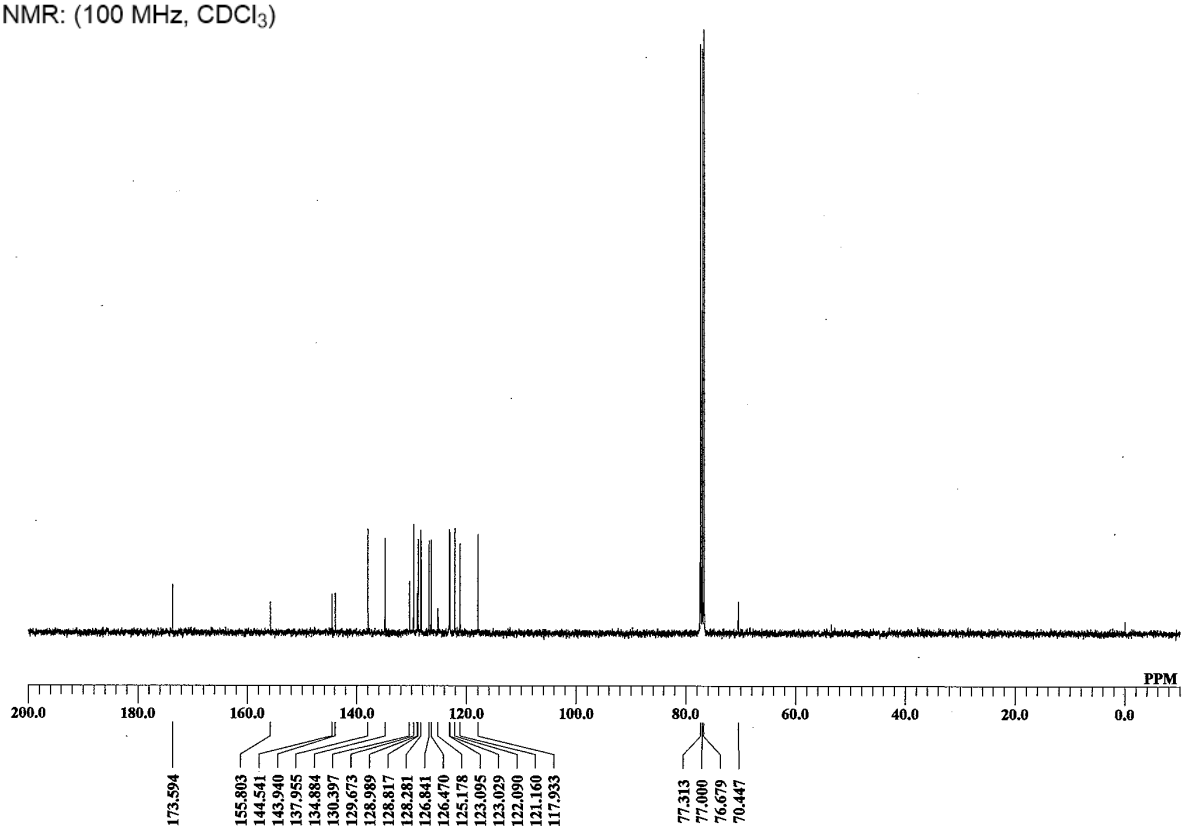

^{1}H NMR: (400 MHz, $CDCl_3$)

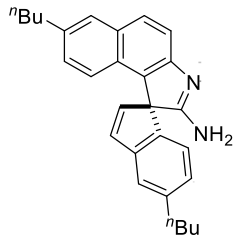

2b

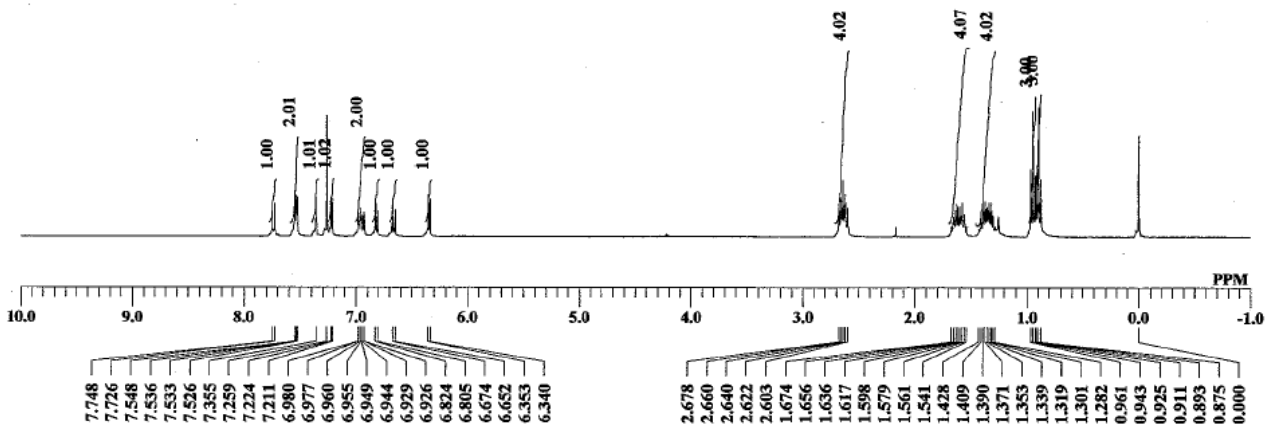

^{13}C NMR: (100 MHz, $CDCl_3$)

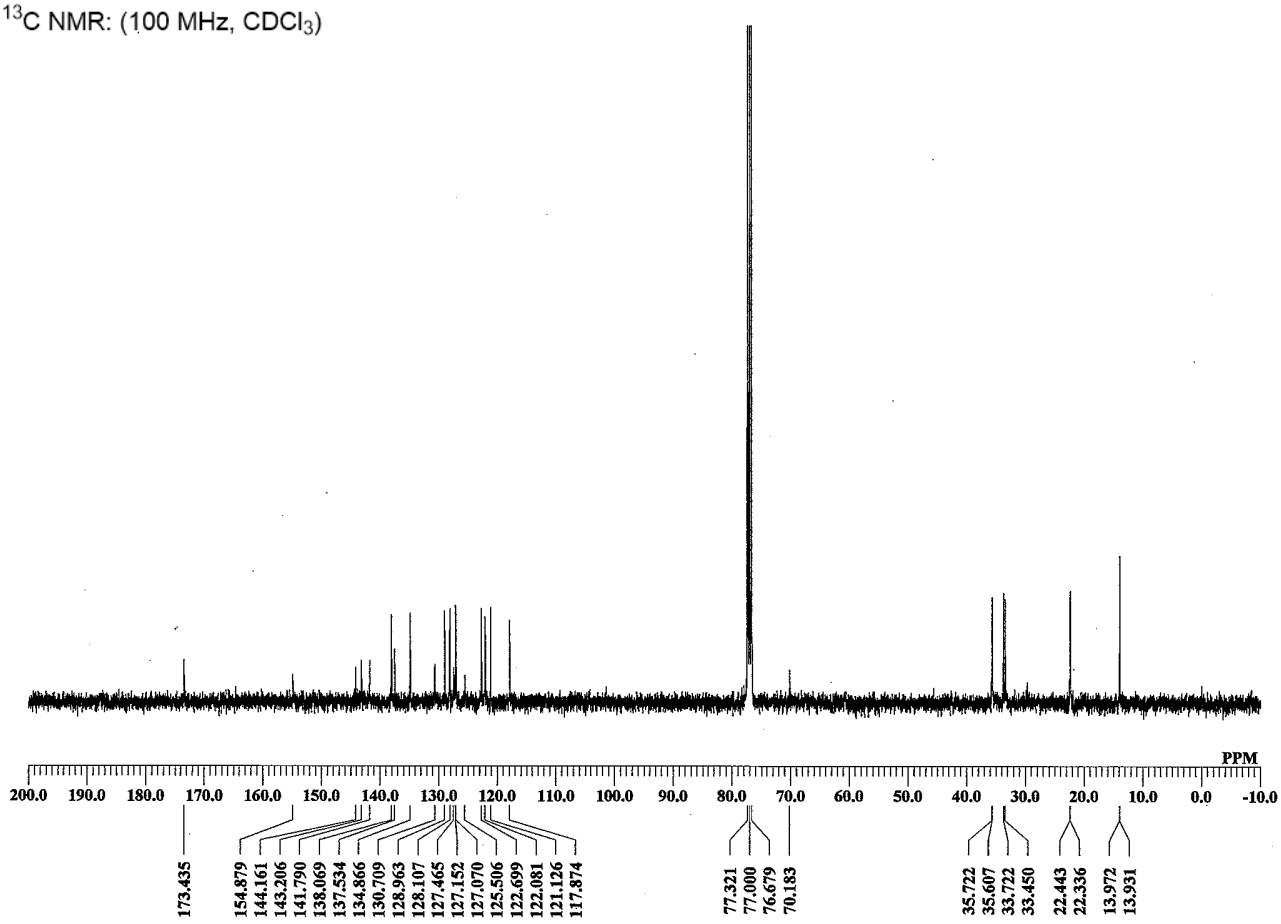

^{1}H NMR: (400 MHz, $CDCl_3$)

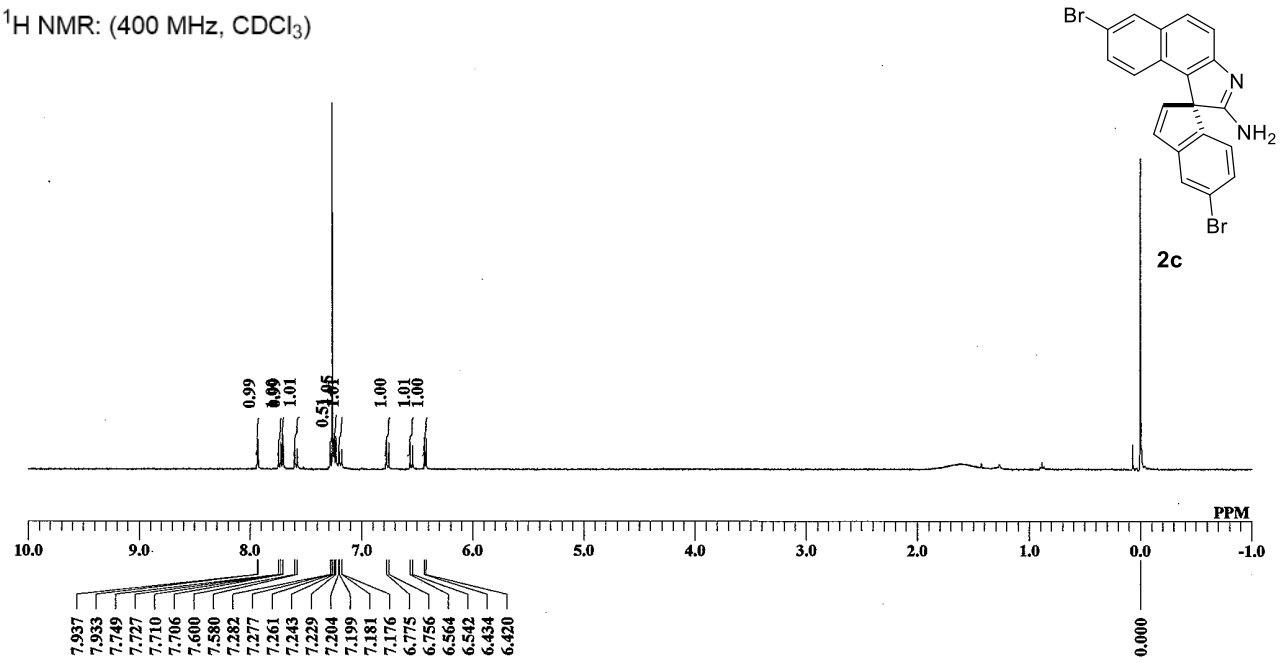

^{13}C NMR: (100 MHz, $CDCl_3$)

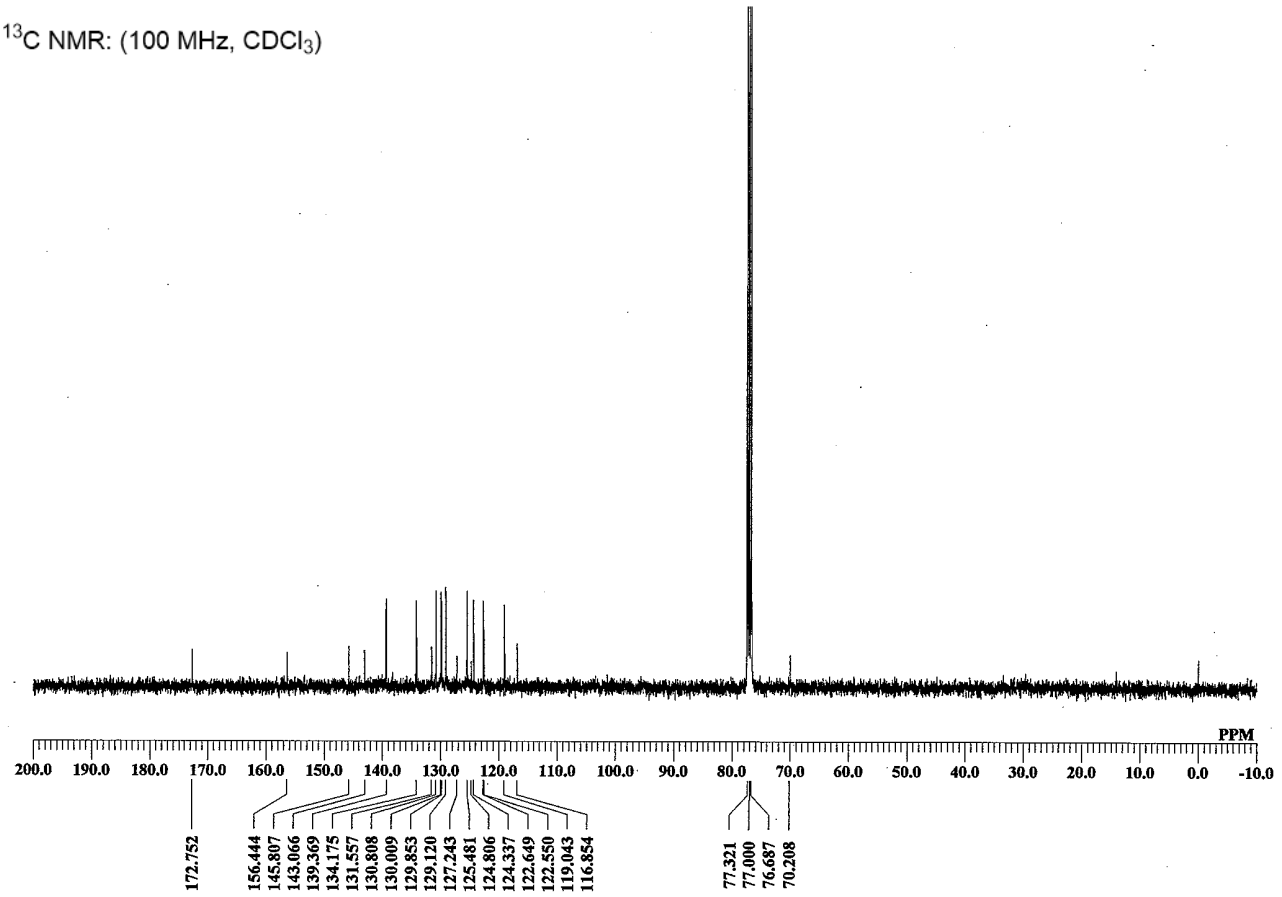

^{1}H NMR: (600 MHz, $CDCl_3$)

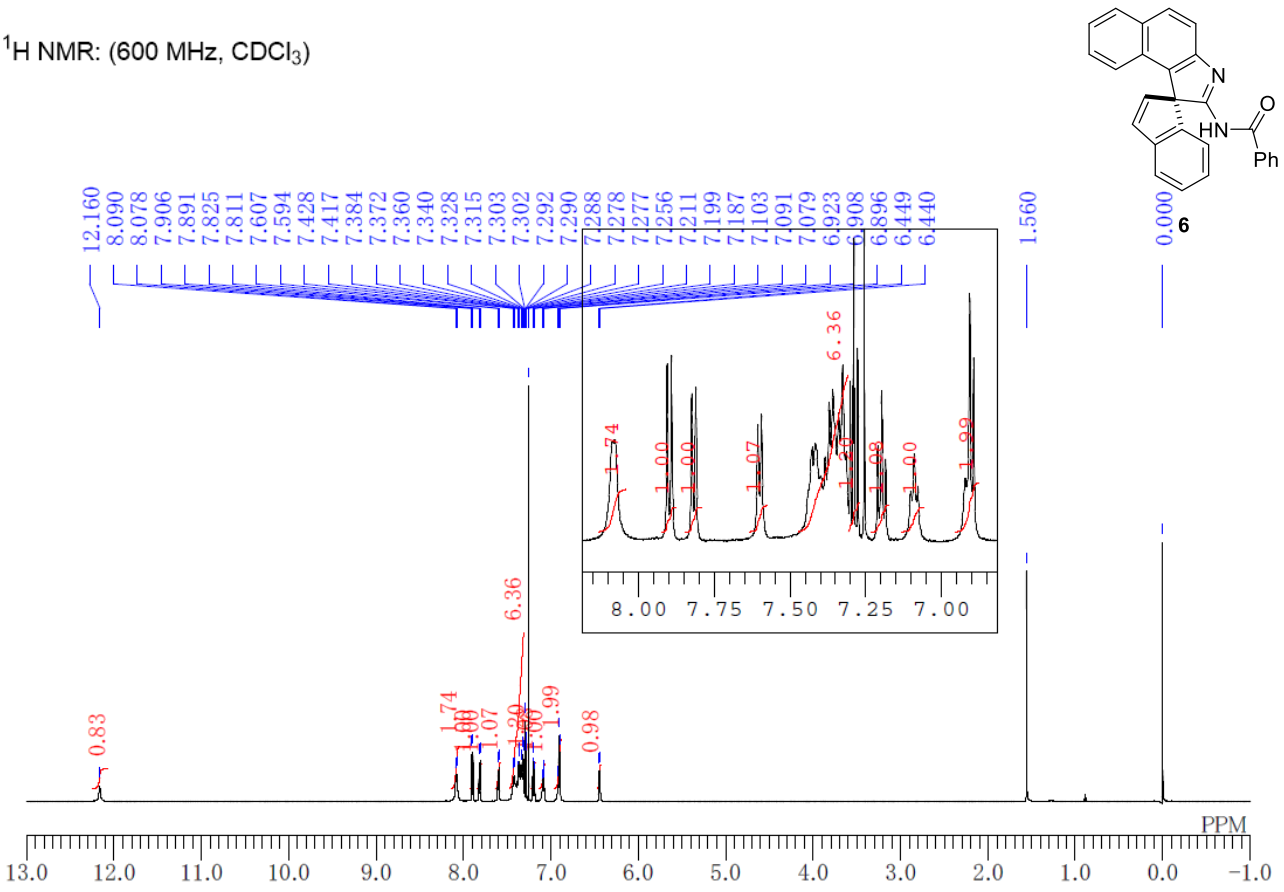

^{13}C NMR: (150 MHz, $CDCl_3$)

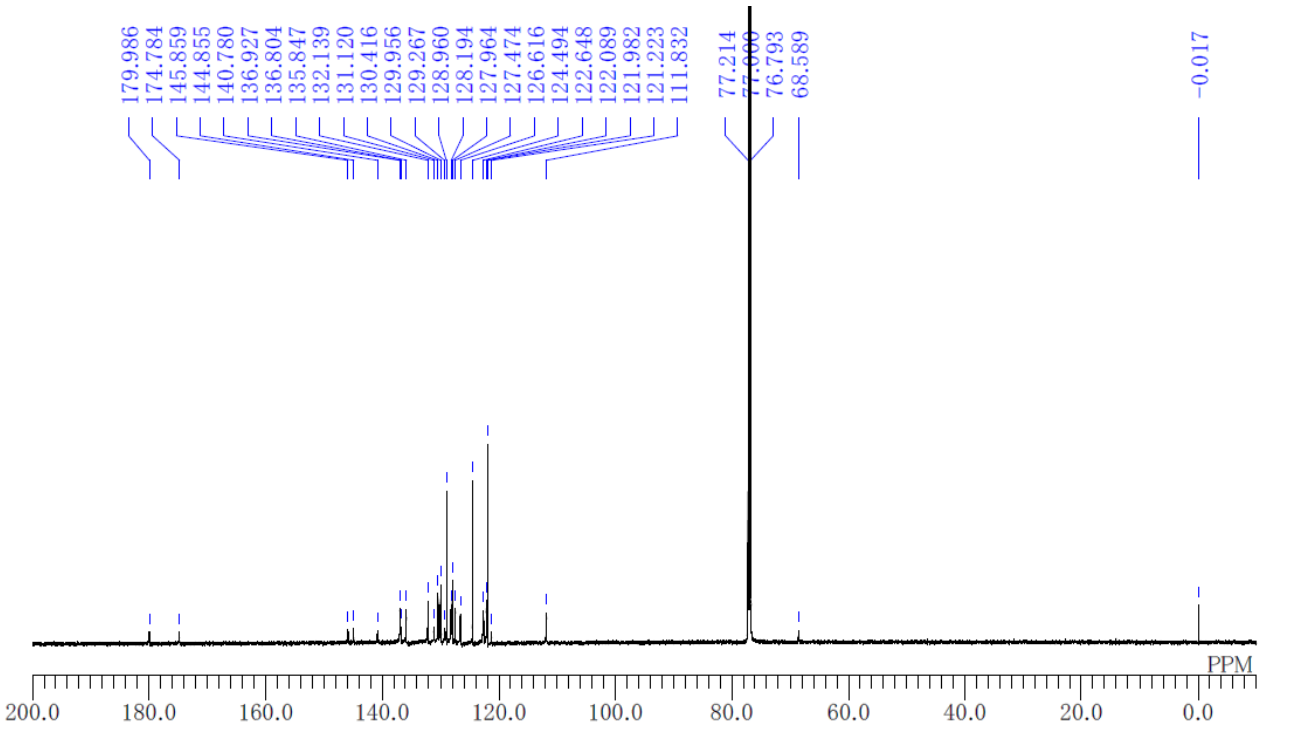

^{1}H NMR: (600 MHz, $CDCl_3$)

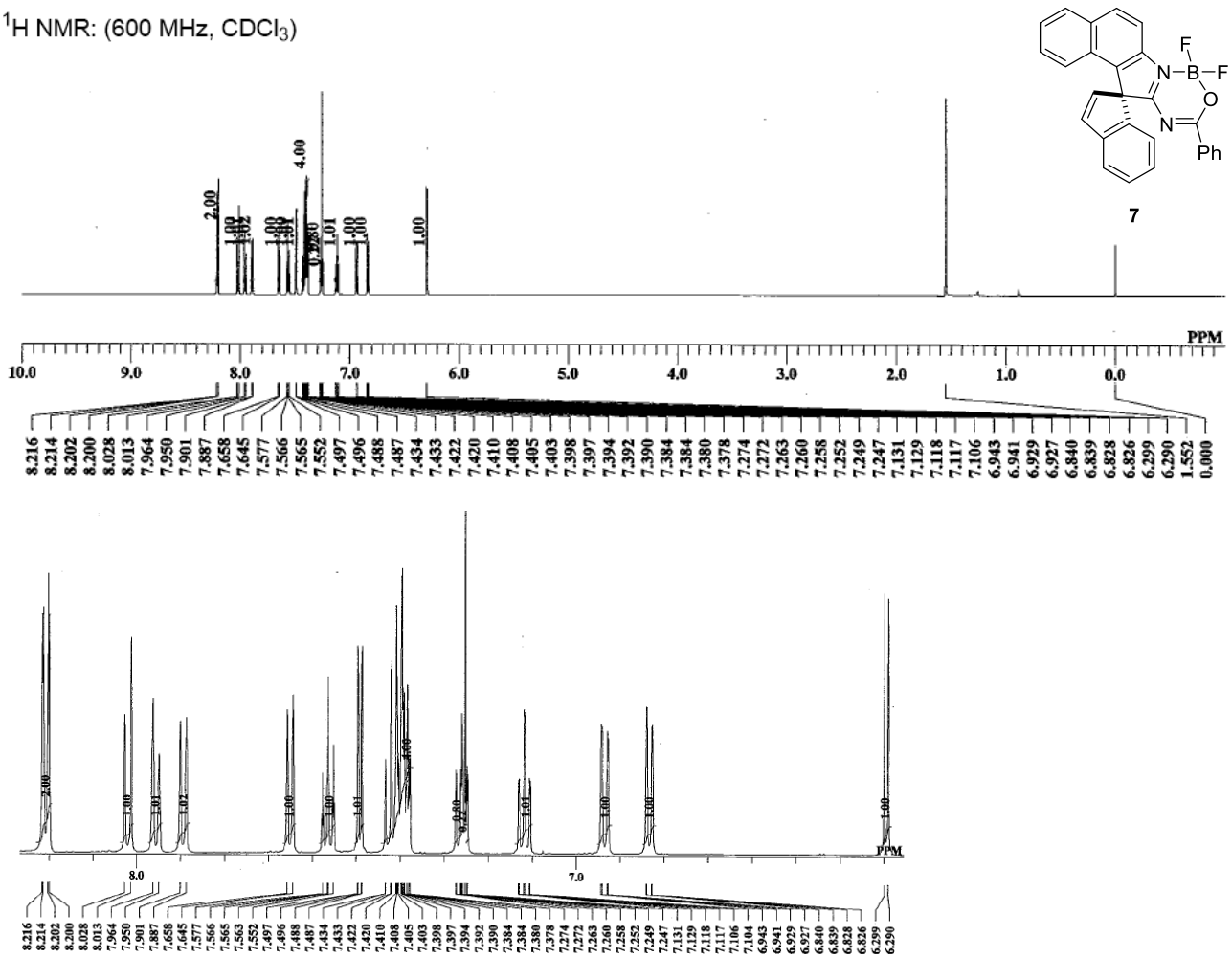

^{13}C NMR: (150 MHz, $CDCl_3$)

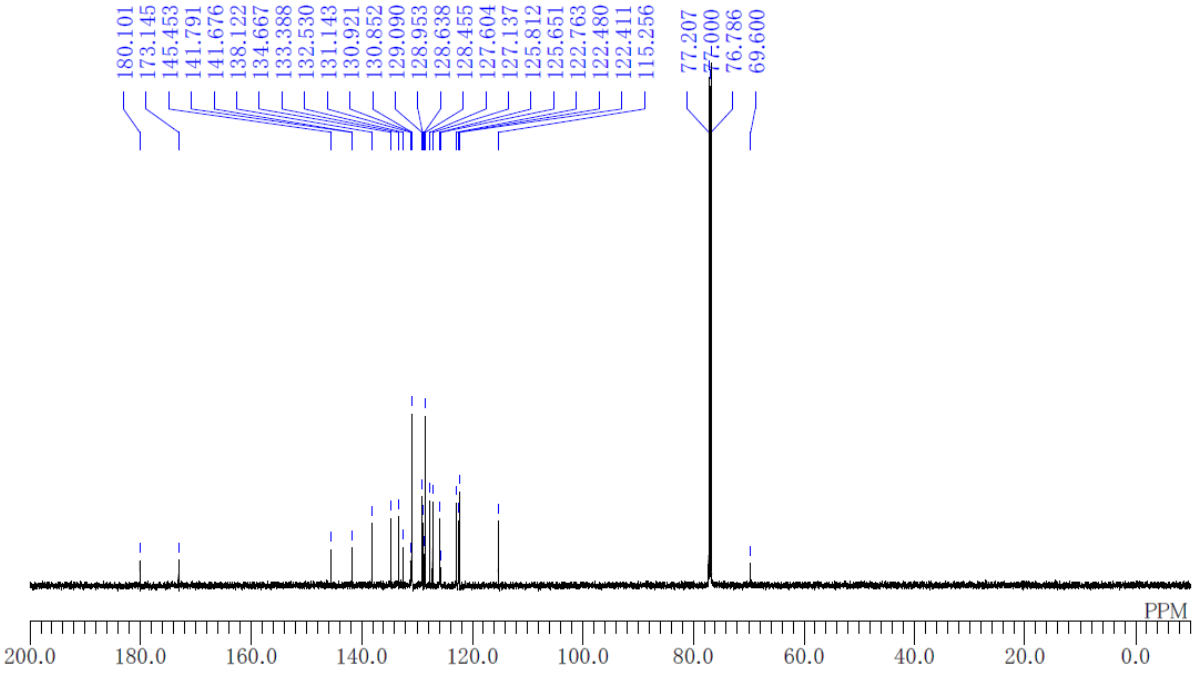

^{19}F NMR: (564 MHz, $CDCl_3$)

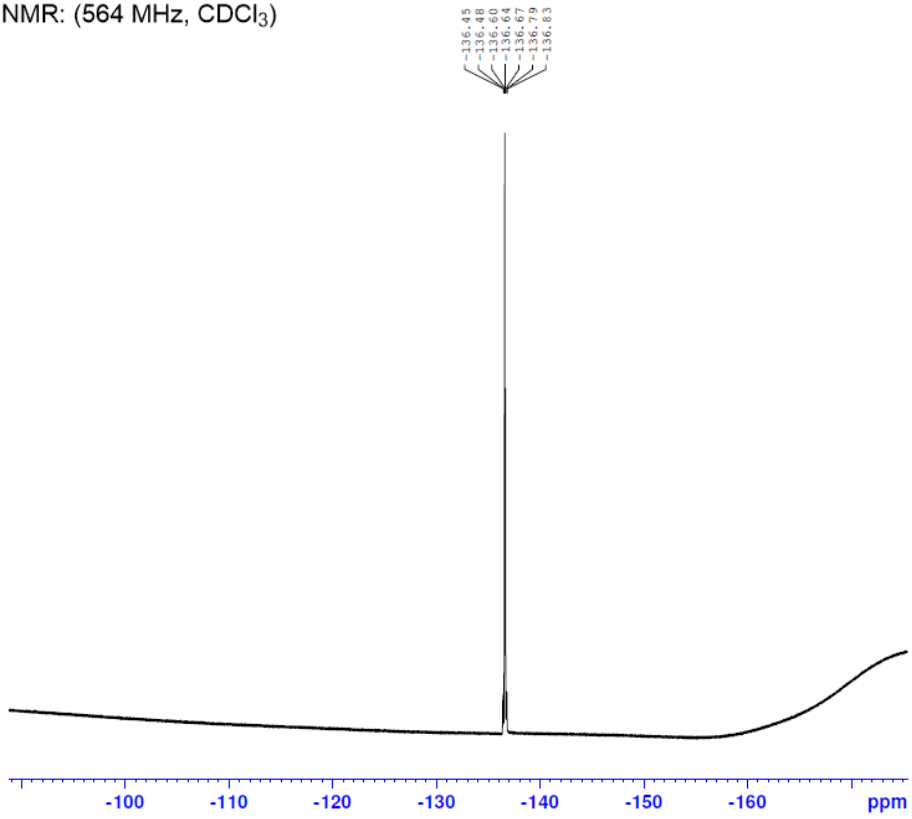


```
Current Data Parameters
NAME         Okazaki_BF2
EXPNO                201
PROCNO                 1

F2 - Acquisition Parameters
Date_           20150826
Time               13.04
INSTRUM            spect
PROBHD   5 mm PABBO BB/
PULPROG         zgflqn
TD              262144
SOLVENT            CDCl3
NS                    16
DS                     4
SWH          100000.000 Hz
FIDRES         0.381470 Hz
AQ             1.3107200 sec
RG                  22.3
DW                5.000 usec
DE                6.50 usec
TE                298.2 K
D1             5.00000000 sec
TD0                    1

======== CHANNEL f1 ========
SFO1         564.6186256 MHz
NUC1                 19F
P1                17.00 usec
PLW1         27.00000000 W

F2 - Processing parameters
SI                262144
SF           564.6870956 MHz
WDW                  EM
SSB       0
LB                0.30 Hz
GB        0
PC                1.00
```

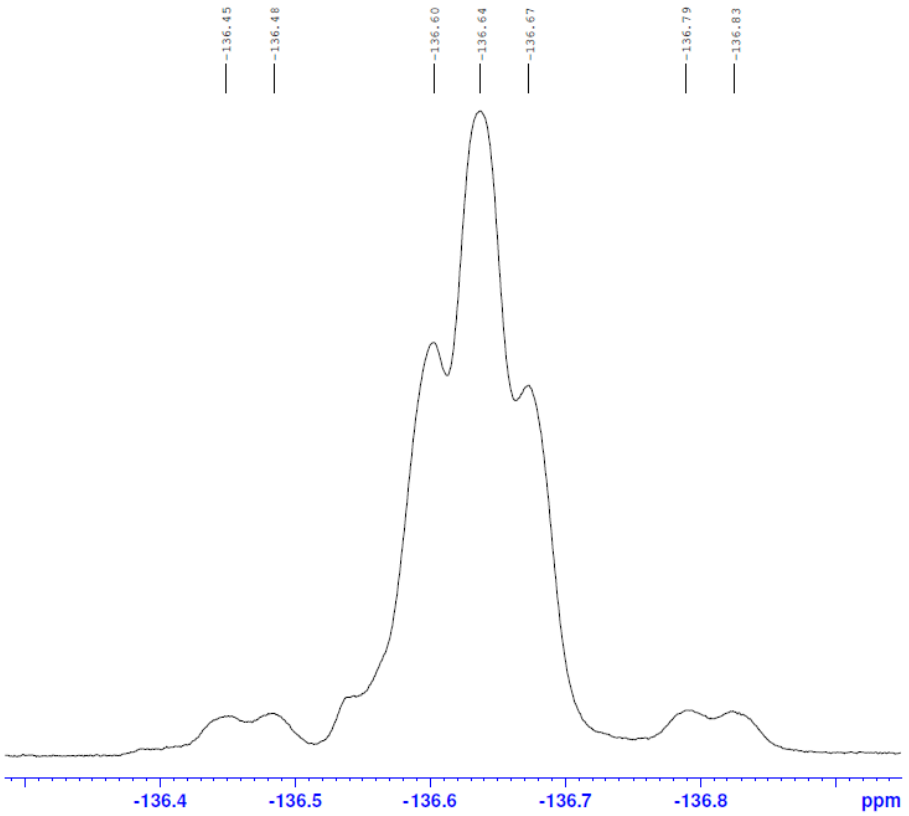


```
Current Data Parameters
NAME         Okazaki_BF2
EXPNO                201
PROCNO                 1

F2 - Acquisition Parameters
Date_           20150826
Time               13.04
INSTRUM            spect
PROBHD   5 mm PABBO BB/
PULPROG         zgflqn
TD              262144
SOLVENT            CDCl3
NS                    16
DS                     4
SWH          100000.000 Hz
FIDRES         0.381470 Hz
AQ             1.3107200 sec
RG                  22.3
DW                5.000 usec
DE                6.50 usec
TE                298.2 K
D1             5.00000000 sec
TD0                    1

======== CHANNEL f1 ========
SFO1         564.6186256 MHz
NUC1                 19F
P1                17.00 usec
PLW1         27.00000000 W

F2 - Processing parameters
SI                262144
SF           564.6870956 MHz
WDW                  EM
SSB       0
LB                0.30 Hz
GB        0
PC                1.00
```

^{11}B NMR: (192 MHz, $CDCl_3$)

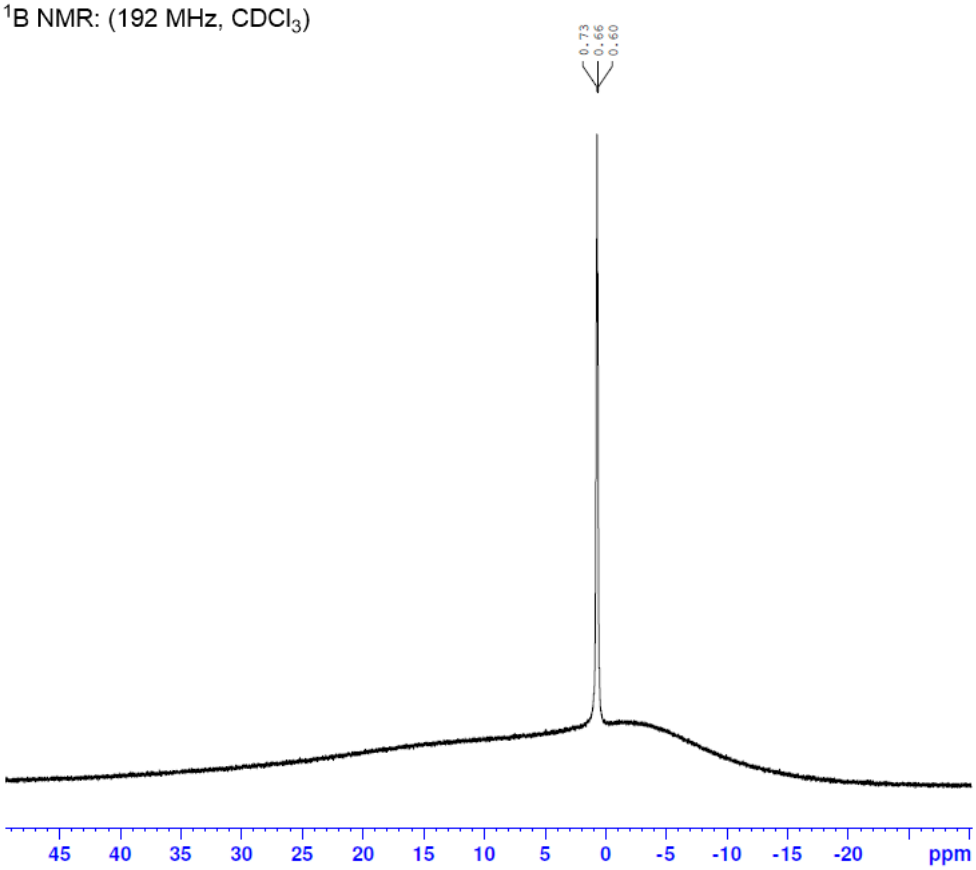


```
Current Data Parameters
NAME         Okazaki_BF2
EXPNO                301
PROCNO                 1

F2 - Acquisition Parameters
Date_           20150826
Time               13.28
INSTRUM            spect
PROBHD   5 mm PABBO BB/
PULPROG               zg
TD                131072
SOLVENT             CDC13
NS                     16
DS                      4
SWH            34722.223 Hz
FIDRES          0.264910 Hz
AQ              1.8874367 sec
RG                185.23
DW                14.400 usec
DE                 6.50 usec
TE                298.2 K
D1             3.00000000 sec
TD0                    1

======== CHANNEL f1 ========
SFO1         192.5513294 MHz
NUC1                 11B
P1                13.00 usec
PLW1        40.00000000 W

F2 - Processing parameters
SI                262144
SF           192.5455765 MHz
WDW                  EM
SSB       0
LB                 1.00 Hz
GB        0
PC                 1.40
```

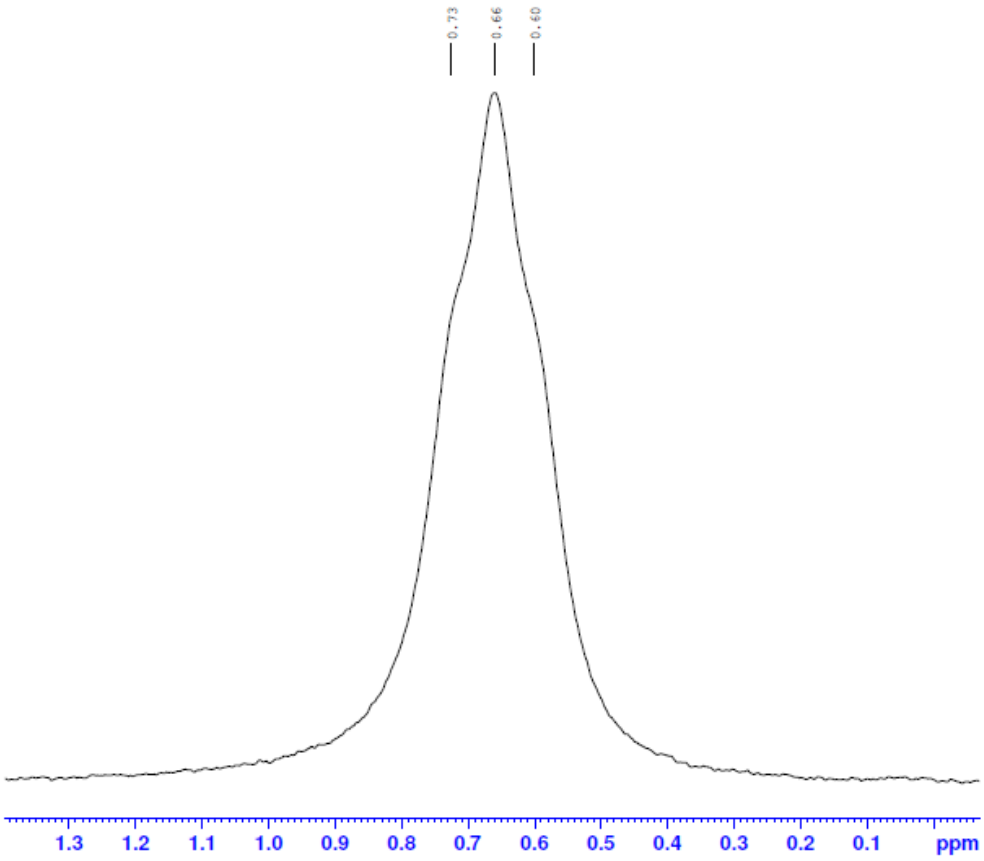


```
Current Data Parameters
NAME         Okazaki_BF2
EXPNO                301
PROCNO                 1

F2 - Acquisition Parameters
Date_           20150826
Time               13.28
INSTRUM            spect
PROBHD   5 mm PABBO BB/
PULPROG               zg
TD                131072
SOLVENT             CDC13
NS                     16
DS                      4
SWH            34722.223 Hz
FIDRES          0.264910 Hz
AQ              1.8874367 sec
RG                185.23
DW                14.400 usec
DE                 6.50 usec
TE                298.2 K
D1             3.00000000 sec
TD0                    1

======== CHANNEL f1 ========
SFO1         192.5513294 MHz
NUC1                 11B
P1                13.00 usec
PLW1        40.00000000 W

F2 - Processing parameters
SI                262144
SF           192.5455765 MHz
WDW                  EM
SSB       0
LB                 1.00 Hz
GB        0
PC                 1.40
```

Chiral HPLC Chart

(Chiralcel OD-H, *i*-PrOH/*n*-hexane 2:98, 1.0 mL/min, 254 nm)

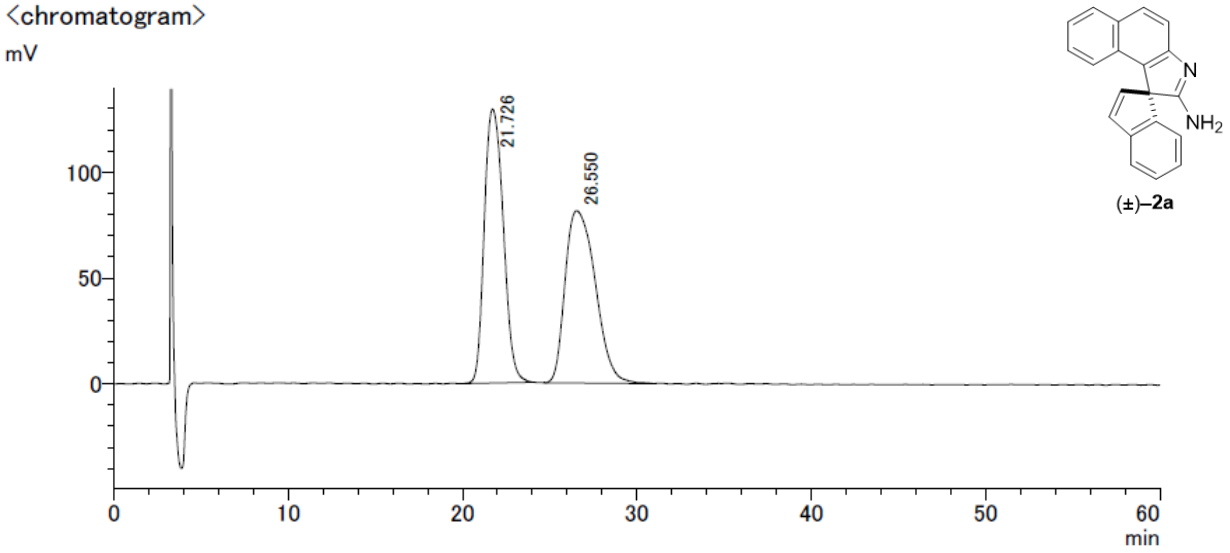

<peak report>

peak#	retention time	area	height	area%
1	21.726	9811839	129452	50.016
2	26.550	9805475	81322	49.984

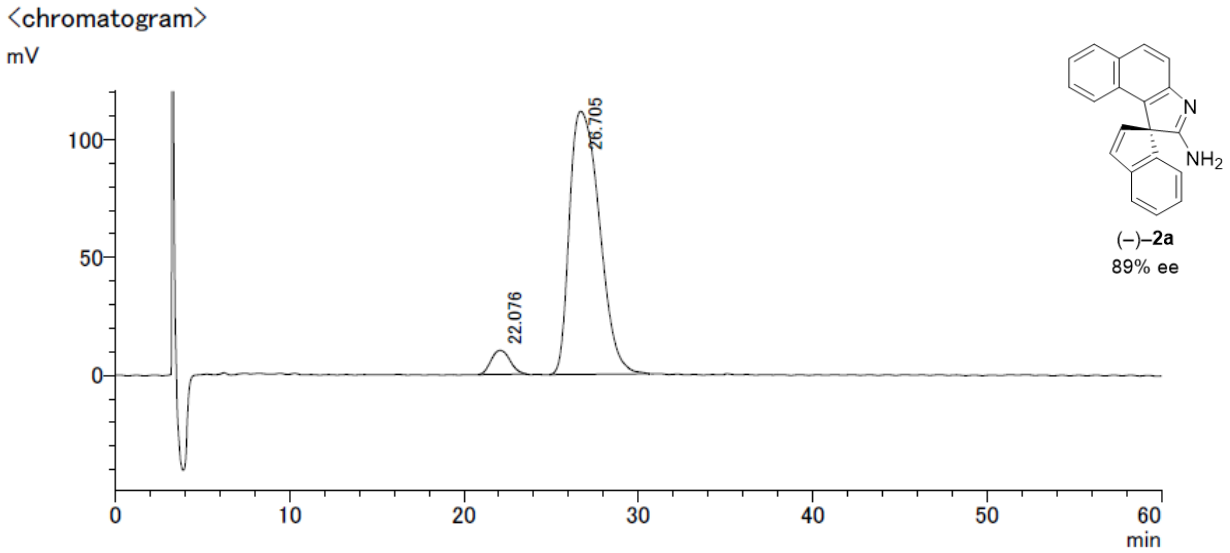

<peak report>

peak#	retention time	area	height	area%
1	22.076	770314	10170	5.458
2	26.705	13342429	111537	94.542

References

S1 M. Vilches-Herrera, J. Miranda-Sepúlveda, M. Rebolledo-Fuentes, A. Fierro, S. Lühr, P. Iturriaga-Vasquez, B. K. Cassels, and M. Reyes-Parada, *Bioorg. Med. Chem.*, 2009, **17**, 2452.

S2 D. Sue, T. Kawabata, T. Sasamori, N. Tokitoh, and K. Tsubaki, *Org. Lett.*, 2010, **12**, 256.

S3 J-X, Chen, Y-Q. Wang, S.-W. Liu, W.-E. Lin, and Z.-P. Chen, *Acta. Cryst.*, 2011, **E67**, o9.

S4 H. Zhao, U. Al-Atar, T. C. S. Pace, C. Bohne, and N. R. Branda, *J. Photochem. Photobiol. A: Chem.*, 2008, **200**, 74.

S5 B. Valeur and M. N. Berberan-Santos, 'Molecular Fluorescence: Principles and Applications,' 2nd edn., WILEY-VCH, Weinheim, 2012.

S6 A. Altomare, G. Cascarano, C. Giacovazzo, A. Guagliardi, M. C. Burla, G. Polidori, and M. Camalli, *J. Appl. Cryst.,* 1994, **27**, 435.

S7 Gaussian 09, Revision A.02, M. J. Frisch, G. W. Trucks, H. B. Schlegel, G. E. Scuseria, M. A. Robb, J. R. Cheeseman, G. Scalmani, V. Barone, B. Mennucci, G. A. Petersson, H. Nakatsuji, M. Caricato, X. Li, H. P. Hratchian, A. F. Izmaylov, J. Bloino, G. Zheng, J. L. Sonnenberg, M. Hada, M. Ehara, K. Toyota, R. Fukuda, J. Hasegawa, M. Ishida, T. Nakajima, Y. Honda, O. Kitao, H. Nakai, T. Vreven, J. A. Montgomery Jr., J. E. Peralta, F. Ogliaro, M. Bearpark, J. J. Heyd, E. Brothers, K. N. Kudin, V. N. Staroverov, R. Kobayashi, J. Normand, K. Raghavachari, A. Rendell, J. C. Burant, S. S. Iyengar, J. Tomasi, M. Cossi, N. Rega, J. M. Millam, M. Klene, J. E. Knox, J. B. Cross, V. Bakken, C. Adamo, J. Jaramillo, R. Gomperts, R. E. Stratmann, O. Yazyev, A. J. Austin, R. Cammi, C. Pomelli, J. W. Ochterski, R. L. Martin, K. Morokuma, V. G. Zakrzewski, G. A. Voth, P. Salvador, J. J. Dannenberg, S. Dapprich, A. D. Daniels, O. Farkas, J. B. Foresman, J. V. Ortiz, J. Cioslowski, and D. J. Fox, Gaussian, Inc., Wallingford CT, 2009.